Direct Drive Hands:
Force-Motion Transparency in Gripper Design

Ankit Bhatia, Aaron M. Johnson and Matthew T. Mason
Robotics Institute
Carnegie Mellon University
Pittsburgh, Pennsylvania
Email: {ankitb,amj1,mattmason}@cmu.edu

Abstract—The Direct Drive Hand (DDHand) project is exploring an alternative design philosophy for grippers. The conventional approach is to prioritize clamping force, leading to high gear ratios, slow motion, and poor transmission of force/motion signals. Instead, the DDHand prioritizes *transparency*: we view the gripper as a signal transmission channel, and seek high-bandwidth, high-fidelity transmission of force and motion signals in both directions. The resulting design has no gears and no springs, occupying a new quadrant in the servo gripper design space. This paper presents the direct drive gripper design philosophy, compares the performance of different design choices, describes our current design and implementation, and demonstrates a fly-by "smack and snatch" grasping motion to show the gripper's ability to safely detect and respond quickly to variations in the task environment.

I. INTRODUCTION

What are hands for? If your answer is that hands are for gripping a wide variety of objects, then you will choose a hand that looks like a vise, to provide a secure grasp over a wide range of object weight and disturbance forces. But a hand can be much more than that, so a better answer may be that hands are for interacting with the environment. While a vise imposes large forces on the environment, it does not react to changes in the environment or comply to avoid crushing a delicate object. The vise is strong, but not smart or interactive. In order for a hand to support a wide range of interactions with the environment, the mechanism must allow force and motion to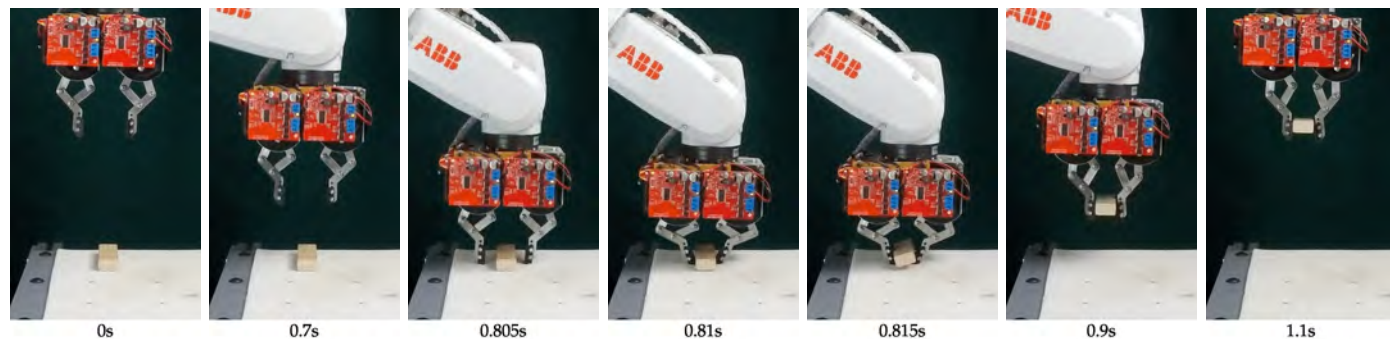 pass between the robot and its environment with the least possible compromise: high bandwidth and high signal-to-noise ratio in each direction. We adapt a term often used in teleoperation and human-robot interaction: "transparency" [18, 16, 25, 39]. It should feel like the mechanism coupling the agent to the task is completely transparent–not there at all.

Most robotic grippers achieve vise-like rigid clamping using a high gear-ratio worm screw or similar transmission. If sustained high clamping force is required, and if actuator torques are limited, a high gear ratio is unavoidable. But as actuator torques improve, lower gear ratios become viable, and gripper capabilities can be expanded to provide a class of interaction that supports a broader range of applications, including unstructured environments and human-robot interaction.

We illustrate the value of direct drive using the example behavior called "smack and snatch" (Fig. 1). The goal is to quickly acquire an object at rest on a table. The table's height is not known precisely. The gripper smacks the table and snatches the object so quickly that the arm need not slow down at all. (A grasp called a "snatch" was demonstrated in [27], using inertial forces to acquire an object without squeezing it). A traditional industrial robot and gripper would have to approach the table very slowly, detecting contact with a force/torque sensor, contact sensor, or by monitoring servo error to avoid crushing the finger into the surface.

The contributions of this work are

- An alternative perspective on gripper function, analysis,

Fig. 1: The DDHand executing the "smack and snatch" behavior. The manipulator is uncertain of the object pose and the table height. The arm accelerates the hand towards the object; fingers detect contact with the table then slide along the surface to locate the object; the arm simultaneously decelerates; the fingers grab the object while the arm accelerates upwards. The grasping maneuver is completed within one second, starting and ending at rest.

design, and behavior;

- A corresponding analysis and comparison of different quadrants in gripper design space (Section III);
- The DDHand—an example device embodying the principles of direct drive gripping (Section IV);
- Demonstration of a DDHand capability for high-speed interaction with the task environment. (Section V)

The paper concludes with some further discussion of implications, including the problems associated with reduced clamping force and how to mitigate those problems.

II. RELATED WORK

Compliance: Most robotic manipulators are intended to produce programmed motions accurately, regardless of the forces encountered. In short, they are stiff and obtain high joint torques by using high gear ratios. High gear ratios also lead to high reflected inertias. That means that the inertia perceived by an external observer would include the motor rotor inertia scaled by the gear ratio squared, which dominates the inertia of the arm structure by a considerable margin. That is all fine if the goal is to produce a programmed motion, regardless of forces encountered. It is a great approach for industrial robotics, where there is virtually no role for online intelligence. All the intelligence is offline, which in turn implies that the task environment must conform to offline expectations. Objects must be of predictable shape and in predictable locations, often referred to as "structured environments."

The limitations of the stiff programmed motion approach have long been recognized, and two approaches have been pursued to produce compliant motion: (1) active compliance using a force/torque sensor, as proposed in, e.g., [8, 51, 29, 35, 17]; and (2) passive compliance between the actuators and the load. The passive compliant mechanism could take many forms, such as a spring [52, 33], a differential [7, 11], or a breakaway clutch [48]. One example is the Remote-Center Compliance (RCC) [52]. Another approach, Series-Elastic Actuators (SEA) [33], involves placing one or more springs directly in series with each actuator.

There is much to say about the merits and limitations of both approaches [53], but the inescapable observation is that both approaches start with a compliant source, the electric motor, then add structure and control to make it stiff, and then add more structure and more control to make it compliant again. The alternative is both obvious and appealing: discard the complexity, weight and expense of all the additional stuff, and rely on the native compliance of the actuator: direct-drive.

Direct Drive Actuation: The appeal of direct-drive has been recognized for at least 30 years [3, 38, 12] but it was not practical at the time. Factory automation dominated the commercial applications, and motors lacked sufficient torque. As applications broaden to include unstructured environments and human interaction, and as actuator torque improves, direct-drive is an inevitable addition to the available manipulation systems.

The earliest investigation of direct-drive actuation was the work of Takeo Kanade and Harry Asada [3]. Applications of direct-drive actuation in end-effector design were subsequently explored [26, 12, 38, 23, 10] but failed to pick up momentum due to lacking torque density in motors. There were products with direct-drive actuation in the 1980s but perhaps the first harbingers of substantial commercial application are now appearing, first in specialized applications [1], and subsequently in general purpose manipulators [15, 14]. As motor technology has improved, the well-known advantages of direct-drive (and low gear ratios more generally) has led to a greater interest in the locomotion community [13, 42, 19, 24, 22]. In particular, [24] contains an overview of the advantages and disadvantages of direct-drive, applied to locomotion.

Hand design and control: There are two main lines of hand technology development: commercial and research. Commercial applications are dominated by pneumatic grippers, simple binary devices lacking the controllability and instrumentation required for reactive manipulation. Several commercial electrically actuated grippers are available, using high gear ratios to develop large clamping forces [31]. The other line of development is robotics research, which has focused on more complex hands. Although there is a long history of research in robotic hands [6], direct-drive has not played a significant role. Supplementing gearboxes with series-elastic actuation and strain gauges have been popular actuation modes for robot effector design. Examples include the Ishikawa Hand [32], the Yale Hand [28] and the recent Dynamic Observable Contact Hand [21]. A survey of robot hand designs can be found in [2], and a discussion of actuation modes and transmissions can be found in [47].

Transparency: We borrow and apply the term "transparency" throughout this paper. The term originated in teleoperation, where it means that the operator feels as if directly present in the task. Teleoperation researchers [18, 16, 25, 39] adopted models and analysis that transform the intuitive "feeling present" notion into conditions on the transmission of force and velocity between operator and task. The direct-drive hand adopts the same idea: that the conditions that provide the "feeling present" experience in teleoperation should also apply to couple the robotic end-effector to the controller. The key is effective bidirectional transmission of information carried by force and velocity signals

III. ANALYSIS OF DIRECT-DRIVE ACTUATION

The central hypothesis of this paper is that a favorable approach to robotic manipulation is to use more reactive interactions with the environment, instead of simply imposing forces unilaterally. In particular, we propose direct-drive actuation to achieve this. What are the properties of this actuation scheme that enable this improvement?

Simple models are generally useful for gathering an overview of the space of actuators [47]. We analyze one such simple model to study the advantages and disadvantage of each transmission type when considering the open-loop torque response.
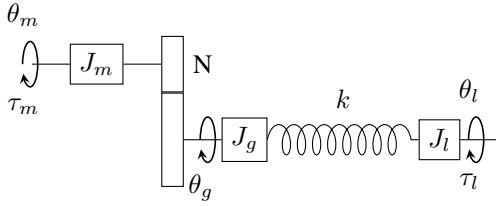
Fig. 2: General model of an actuator. This model is used to describe a continuum of actuator configurations varying from direct-drive to series-elastic with gearing.

A. Models of Actuator Transmission

Actuation schemes for servoed robotic grippers can be broadly divided into three categories:

- geared actuation with series-elastic elements;
- geared actuation with strain-gauges;
- direct drive actuation.

The demarcation between these categories is blurry; they lie on a continuum as shown in Fig. 4. For example, a strain gauge is essentially a stiffer series elastic element and an ideal direct drive can be approximated by a series-elastic actuation scheme with infinite spring stiffness and a unit gear ratio. To elucidate the inherent differences between these schemes, we use a general model of an actuator and transmission that includes each as a special case (Fig. 2). From this model, we examine the equations of motion, scaling of the reflected inertia, and the torque response of the different actuation schemes. Conclusions based on this model are discussed in Section III-B.

The model consists of three inertias, J_m, J_g, J_l, corresponding to the motor, gearing, and linkage, respectively, a gear ratio N with efficiency η, and a spring stiffness k (which represents either the series-elastic element or the strain-gauge). The coordinates θ_m, θ_g, and θ_l represent the angular position of the output of the motor, gearbox, and linkage, respectively. Finer details like modeling gear backlash are ignored for now to avoid unnecessary complexity. The equations of motion for this system are,

$$\left(N^2 J_m + J_g\right) \ddot{\theta}_g + k(\theta_g - \theta_l) = \eta N \tau_m, \qquad (1)$$
$$J_l \ddot{\theta}_l + k (\theta_l - \theta_g) = \tau_l. \qquad (2)$$

The term $\left(N^2 J_m + J_g\right)$ in Equation 1 indicates that the *reflected inertia* of the motor's rotor inertia after the gearbox is scaled by N^2. Even if the inertia of the motor's rotor is small, with a high gear ratio the reflected inertia tends to be quite large. On the other hand, with a low gear ratio a larger motor may be required to achieve the desired force output, making the rotor inertia itself larger.

So how does the motor inertia scale with torque? There is some disagreement on this point. For a fixed motor, adding a gear ratio increases the torque by N but the inertia by N^2. To get the same increase in torque by instead increasing the size of the motor, the inertia must increase by a factor between N and N^2 depending on what is held constant [44, 42, 43, 24].

Empirically, the scaling law that is seen in data from motor manufacturers, as shown in Fig. 3, lies somewhere in the middle. Whichever model is considered, the effect is still favorable when compared to the N^2 scaling that gearboxes impose, especially when the added inertia and reduced efficiency from gearbox itself is considered. That is, to achieve the same output torque, choosing a larger motor results in a lower reflected inertia than adding a gearbox.

B. Implications of Direct Drive

Based on this simple model of actuator transmission, there are several important implications of direct-drive actuation for hand design: *transparency*, *force bandwidth*, and *speed*. This is in addition to the *mechanical simplicity* that comes from eliminating the gearbox.

A low reflected inertia implies that the actuator is more *transparent*. That is, when a finger impacts something the loss in energy due to the motor decelerating is not as high. Equivalently, the impact does not impart as large an impulse on whatever the finger has impacted, allowing for a lighter touch.

With lower reflected inertia the finger can accelerate and decelerate faster, allowing for higher bandwidth force, velocity, or position control. Similarly, thinking of the actuator as a sensor, the input bandwidth is also higher as the world can more easily accelerate the lower inertia. Thus, the robot can feel what it is touching faster, and without the compounding issues of low-efficiency and backlash in the transmission. In some cases, the gearbox may not be back-drivable at all, precluding any sensing of the world at the motor.

The notion of *force bandwidth* is important for manipulation, and warrants a more precise definition. Reaction time of the hand to external disturbances is determined by the speed with which a force can be sensed and servoed. The choice of stiffness in the mechanism affects this bandwidth. The transfer function from motor torque to load acceleration (assuming zero load torque) is identical to the transfer function from the load torque to motor acceleration (assuming no applied motor torque). It is
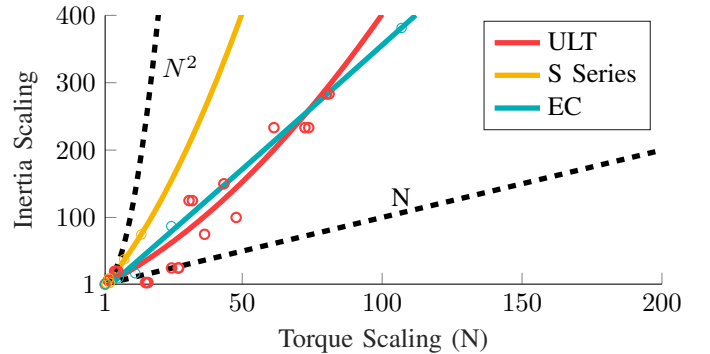

Fig. 3: Scaling laws for three commercially available motor series are compared against the N^2 scaling law for gearboxes. The ULT series motors are manufactured by Celera Motion, the S series by Aerotech and the EC motors by Maxon.
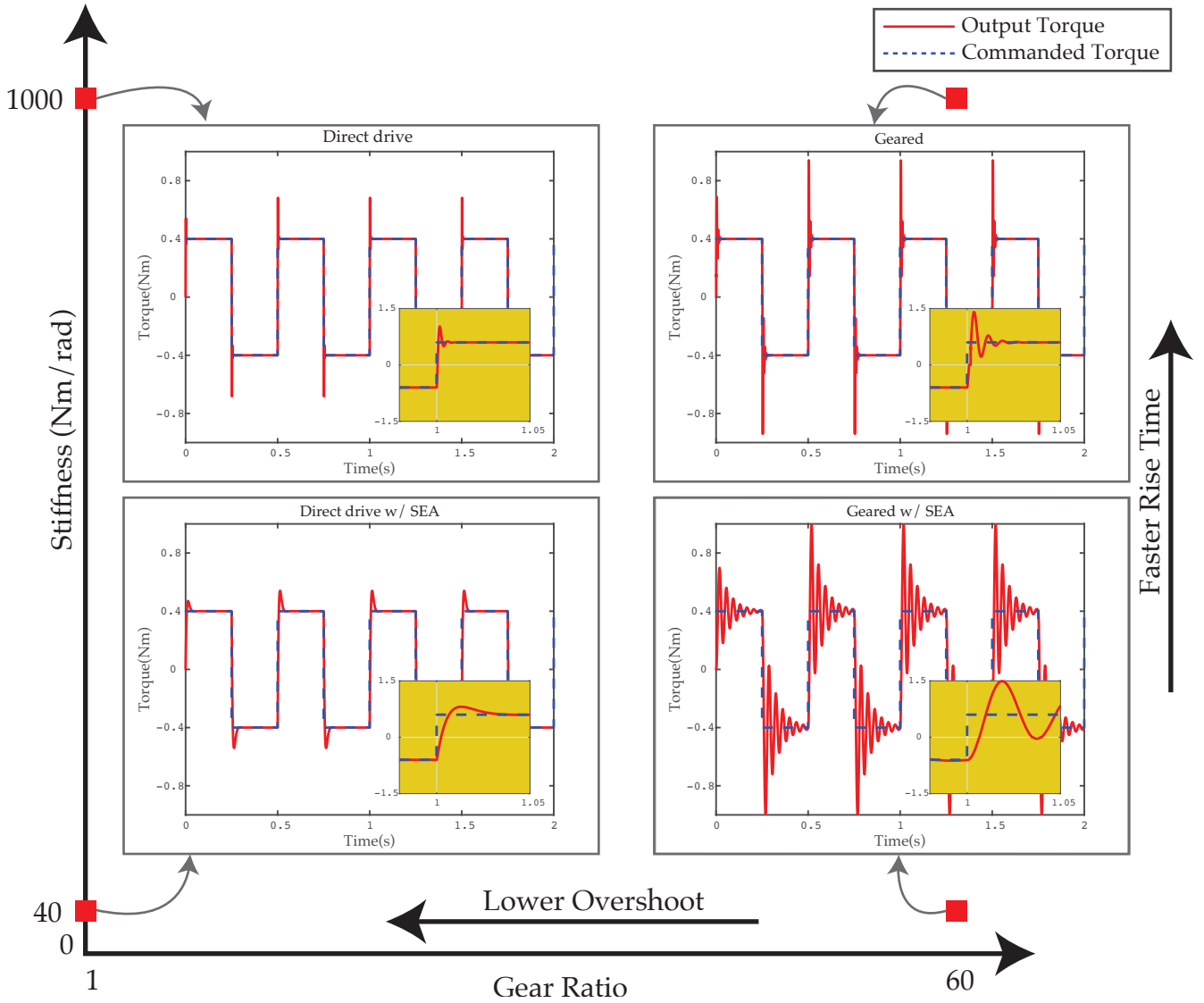
Fig. 4: Open-loop torque response of a simulated actuator with a locked output to a square wave. The yellow inset plots are zoomed in to show the response to a single step. In particular, note the faster rise time as stiffness is increased and the reduced overshoot as gear ratio is reduced. The force bandwidth, the speed at which force can be sensed and servoed, is highest with the direct drive actuation scheme.

given by,

$$\frac{\ddot{\theta}_l}{\tau_m} = \frac{\ddot{\theta}_m}{\tau_l} = \frac{\eta N k}{(J_m N^2 + J_g)J_l s^2 + k(J_m N^2 + J_g + J_l)}. \quad (3)$$

This system resembles a mass-spring system $m_e \ddot{x} + k_e x = F$ with effective mass $m_e = (J_m N^2 + J_g)J_l$ and effective stiffness $k_e = k(J_m N^2 + J_g + J_l)$. The transfer function for this system is given by $1/(m_e s^2 + k_e)$. The natural open-loop frequency ω is given by

$$\omega = \frac{1}{2\pi}\sqrt{\frac{k_e}{m_e}} = \frac{1}{2\pi}\sqrt{\frac{k(J_m N^2 + J_g + J_l)}{(J_m N^2 + J_g)J_l}} \quad (4)$$

$$= \frac{1}{2\pi}\sqrt{k\left(\frac{1}{J_m N^2 + J_g} + \frac{1}{J_l}\right)} \quad (5)$$

The natural frequency is proportional to $\sqrt{k}$ (where k is the spring stiffness); so the higher the stiffness, the higher the bandwidth. Additionally, reducing the reflected and gearbox inertias $(J_m N^2 + J_g)$ also increases the bandwidth.

To evaluate the improvement in force bandwidth, in Fig. 4 we show simulation results of a higher-fidelity model. This model includes the effects of backlash and structural damping. The geared simulation is based on the Maxon EC-20 flat motor (serial number 241916) and a N=60:1 gearbox. For the direct drive simulations, we scale the torque of the motor by N and the inertia of the motor by $N^{1.5}$ to keep the torque output of both configurations comparable. An experimental comparison of these actuator schemes can be found in [20].

With this model we test the effect of stiffness and gear ratio

Fig. 5: Design of the two-finger parallel DDHand. The Motor drivers are not shown.

on the open-loop torque response of the actuator to a square wave in a locked output state. Moving from unit gearing to a ratio of 60, the overshoot increases due to the increased reflected inertia. Increasing stiffness from $40\,\mathrm{N\,m\,rad^{-1}}$ to $1000\,\mathrm{N\,m\,rad^{-1}}$ improves the rise time of the system due to the reduced delay required to compress the spring.

Higher speed is another byproduct of direct drive actuation which is well motivated by industry's need for faster cycle times. As the gear ratio moves towards unity, it unlocks access to higher speed ranges. Even if the motors are designed to work at a fixed speed, a direct-drive architecture allows the finger to move much faster than in a geared setting. Higher bandwidth, in addition to higher top speed, means that the hand can more quickly change the applied torque. This higher speed is, of course, a direct trade-off with peak *stall torque* for a given motor with different gearing.

Finally, the issue of *mechanical simplicity* is not addressed by this simple model. Beyond the additional mass and losses due to inefficiencies, gearboxes and springs tend to involve multiple moving parts that wear, deform, and can break. Eliminating these components simplifies the design and eliminates possible points of failure. Gearboxes do not add any power but take up space and add mass, and so the overall actuator power per unit volume or mass is improved by eliminating them (note that torque density may be higher or lower as a larger motor is needed.)

IV. DESIGN OF THE DDHAND

The design of the Direct-Drive Hand is shown in Fig. 5. The finger modules, inspired by the Minitaur [24] and other robots [23, 10], feature a parallel 5-bar linkage connected to two brushless gimbal motors. Finger modules can be arranged into parallel and spherical hand designs to support a variety of tasks. A two finger parallel configuration is presented here.

The linkage design allows the finger to squeeze with twice the force that one motor can produce and reduces the torque requirement on the motors. Placing both motors at the base of the finger ensures that the linkage inertia is low and the fingers can be accelerated or decelerated quickly.

Each finger module has two T-Motor GB54-2 brushless DC (BLDC) gimbal motors [45]. A continuous torque of $0.3\mathrm{N\,m}$ (at 24V) per motor has been experimentally verified. With a finger length of $10\mathrm{cm}$, the DDHand can produce a force of 6N at the fingertips. We chose gimbal motors for three reasons: (1) The are low cost and easily available due to the boom in DIY hobby drones; (2) gimbal motors are wound for high voltage, low current applications (producing less heat and enabling the use of smaller MOSFETs); and (3) they are designed for gimbals which are mostly operated at close to zero speed. The low speed is suitable for manipulation as it is rather unlikely that these motors will be required to spin at speeds higher than 500rpm.

Each finger module is controlled by a custom BLDC motor driver developed in the lab. The drivers are based on the InstaSPIN Field-Oriented Control (FOC) technology from Texas Instruments [46] using two F28069M launchpad and four BOOST-XL DRV8301 booster packs. Each controller module has two three-phase drivers which can output a continuous current of 10A on each driver. Position feedback is achieved with an on-axis magnetic encoder from RLS, which, along with a diametrically polarized magnet, provides 12-bit absolute position sensing. These boards are powered with 24V and communications are handled by a micro-controller on each driver via Controller Area Networking (CAN) bus at 1kHz. The CAN bus can support up to three finger modules at this frequency. The communication rate will suffer on the addition of more finger modules. In future iterations, the control electronics will be integrated into the chassis of the DDHand.

A Proportional-Derivative scheme is used for position control of each motor. The output current is tracked by a FOC loop. Both controllers take the filtered encoder position and velocity as feedback. The hardware interfaces with a computer running Robot Operating System (ROS) and is compatible with ROS Control [34]. This gives us the ability to run real-time controllers alongside ROS on the same computer. This enables quick deployment of planners and controllers as well as real-time controller switching and gain scheduling. For the experiments in this paper, we are only using this component for trajectory tracking with interpolation.

The linkage plays an important role in enhancing the capability of this hand, though a study on the design is outside the scope of this paper. The linkage used in the current design is empirically chosen to allow parallel grasps of large and small objects and some variability in the finger angle to enable pinch grasps. See [24, 4] for a discussion of linkage designs.

The mechanical simplicity of this robot hand shows in its bill of materials. The prototype hand has a parts cost of under $1000 in single quantity. This compares favorably with existing grippers as there is no gearbox or series spring to purchase.

| Design Parameters	Value
Rated Continuous Torque (per motor)	0.3N m
Force at Fingertip	6N
Maximum Speed (tested)	200rpm
Rated Voltage	22.5V
Operating Voltage	24V
Motor Driver Continuous Current	10A
Communication Protocol	CAN @ 1kHz
Mechanical Bandwidth	$\geq$12Hz
Degrees of Freedom	4
Parallel Stroke	90mm
Weight	0.9kg
Motor Weight (per motor)	0.18kg
Encoder Resolution	4096cpr
Parts Cost	$\sim$\$1000

TABLE I: Specifications for the DDHand
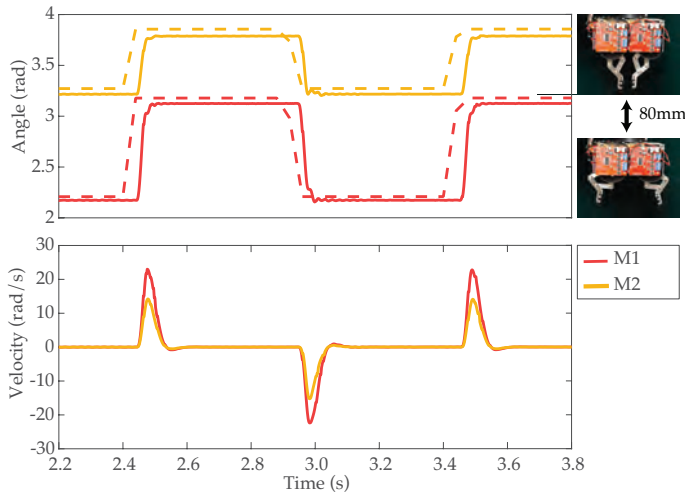
Fig. 6: A step response of one finger module of the DDHand showing the angular position and velocity of the motors. The dotted lines show the commanded positions. The delay seen between the command and response of the motor captures the round trip latency for CAN communication. The lack of an integral gain results in a small steady-state error.

V. EXPERIMENTS

A. Step Response

To demonstrate the enhances in speed and bandwidth of the DDHand, an step input of 80mm is commanded in the parallel grasp mode to the finger modules (Fig. 6). The position and velocity of both motors in one finger module is shown. The motors have a communication delay of approximately 0.05s and a rise time of 0.03s. A steady-state error is seen due to the lack of an integral gain on the motors. This choice was intentionally made to more accurately model the motors as a spring-damper system.

Due to the low reflected inertia, the DDHand can achieve high bandwidth control for dynamic manipulation. A conservative estimate for the bandwidth of the system can be obtained from the rise time [30] as,

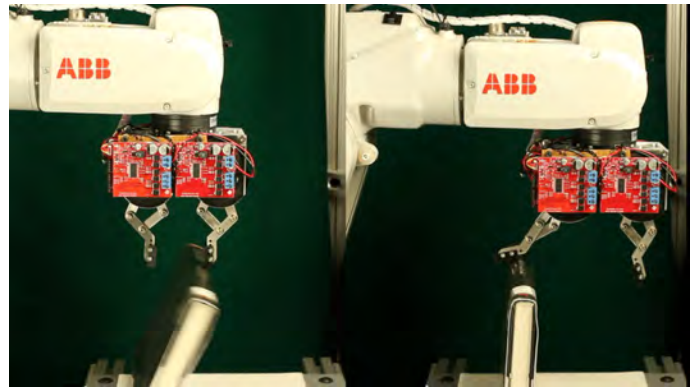$$B = \frac{0.35}{t_r}. \tag{6}$$

Fig. 7: The effect of a transparent finger on an unstable object. In the case of the stiff gripper (left: DDHand with high gains), the book topples. A transparent gripper (right: DDHand with the motors off) is able to maintain contact with the book and prevent toppling.

With this relation, the bandwidth of the hand is estimated at 12Hz. In comparison, the Schunk gripper WSG50 [41] has a stroke length of 55mm, with a maximum speed of 420mm s^{-1} and a maximum acceleration of 5000mm s^{-2}. This means the Schunk gripper takes 0.17s to cover 35mm at max acceleration. Using the above relation, the bandwidth estimated for the Schunk gripper is approximately 2Hz.

B. Transparency and Variable Impedance

If a robot gripper has to interact with an fragile or unstably balanced object like an empty bottle there is a danger that the object will be broken or toppled. This is because there is no way to manage the impulse imparted by the high reflected inertia of the motor rotors through the gearbox. Even if a spring is used, it is generally preferred to use a spring with higher stiffness to preserve the quality of position controller and apply high grasping forces. In contrast, the low reflected inertia of the DDHand mitigates this impulse mechanically. Fig. 7 shows frames from such a contact with a book standing on its edge. When the robot approaches the book with a stiff position controller, unsurprisingly, the book topples. However, if the robot turns off the motors (zero commanded stiffness) the fingers can comply to the book maintaining its vertical state. The transparency also allows for variable impedance control. Varying the PD gains allows us to control the stiffness and damping of the fingers.

C. Smack and Snatch

To begin this task, the robot arm approaches a small object on a table at high speed. The position of the object and height of the table are not known exactly. The fingers make contact with the table first, but their low mass and low reflected inertia ensures that the impulse is low and the hand does not get damaged. When the hand detects the contact the arm's motion can be altered by an upward acceleration that slows and eventually reverses the approach. While the arm is still in motion, the fingertips can track the table surface as they close,
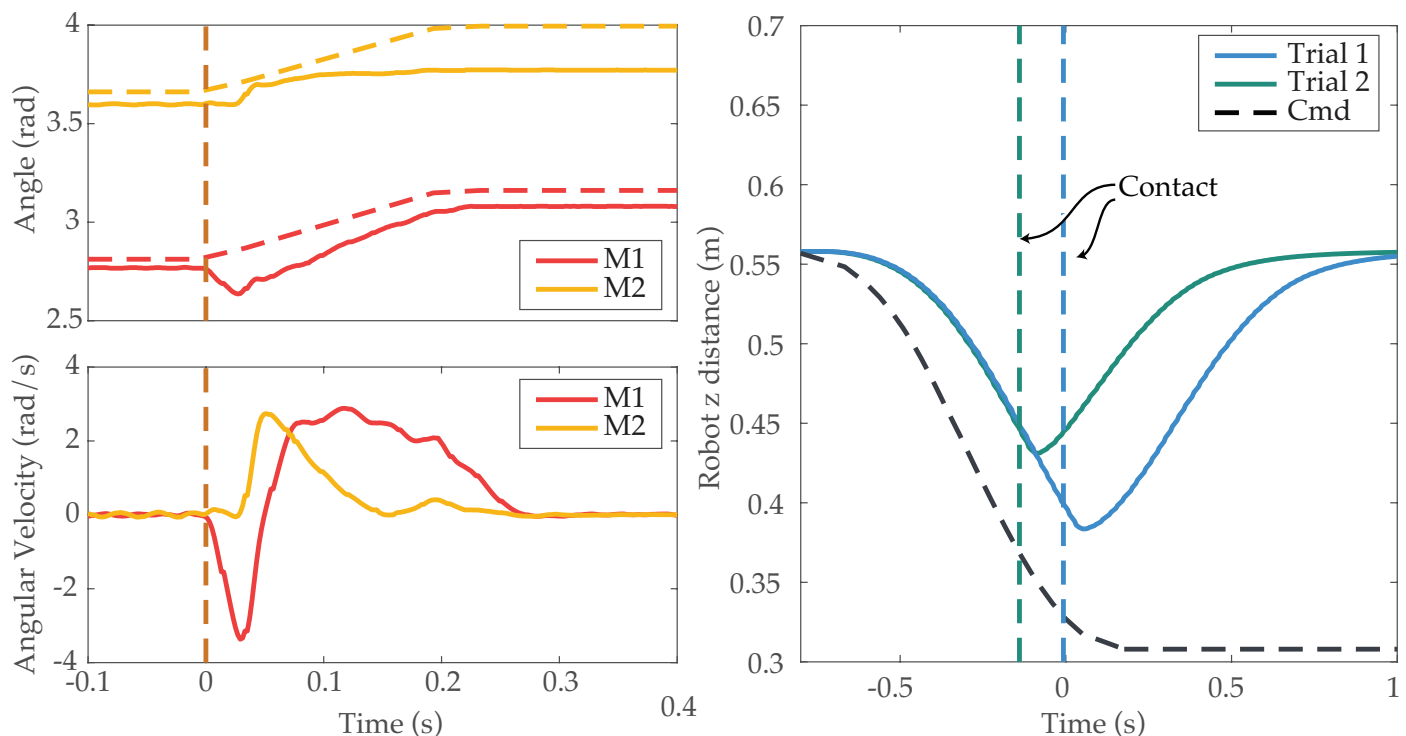
Fig. 8: Left: Evolution of the joint angles of one finger as it makes contact with the surface and begins the snatch behavior. Right: The evolution of the Z coordinate of the robot tool frame. The two trials show the behavior with two different table heights. For all plots, the dotted lines are the commanded reference trajectory.
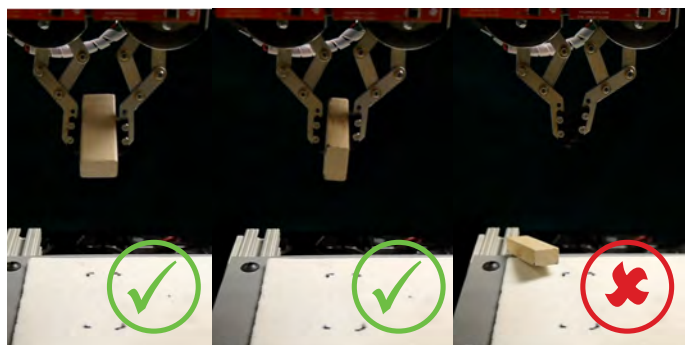

Fig. 9: The figure shows the final state of the block in three out of fifty trials. The first two figures from the left show successful grasps and the rightmost figure shows a failure.

and continue to monitor force to detect contact with the object. The behavior is implemented with an ABB IRB120 robot and the DDHand. The dynamic nature of this behavior requires the control and execution of trajectories on the hand and the arm to be tightly coupled. To achieve the tight timing requirements, the arm is controlled via its Externally Guided Motion (EGM) interface with a communication rate of 250Hz with a 25ms latency. The latency combined with the finite deceleration of the arm require the fingers to be able to absorb the impact forces. During this deceleration, the arm travels approximately 13mm. This travel is absorbed by the fingers. Post-impact, a manually

coded trajectory is executed on the hand with maximum torque limits to execute the snatch phase of the grasp.

A stop motion image sequence is shown in Fig. 1. The behavior is designed to be agnostic to the height of the object. The results from executions at different table heights is shown in Fig. 8.

The smack and snatch behavior was repeated fifty times to get a preliminary estimate of robustness. All fifty trials is included in the video attachment accompanying this paper. A trial was labeled successful when the block transitioned from its initial state to a stable pinch grasp in the hand. The final pose of the block is ignored and can lie in one of two configurations as shown in Fig. 9. Out of fifty attempts, the behavior was successful forty-three times and failed to grasp the block seven times (success rate of 86%.) The failures may be attributed to two factors:

1) On compression of the fingers in the approach phase, a part of the energy is transferred to the table as spring potential energy. This energy, when released, causes an upward velocity of the block making the grasp unstable.
2) If the object is not centered within the fingers, the momentum of the finger that touches the object first is partially transferred to the block. This causes the block to bounce around between the fingers.

These failure modes are equally likely. Out of seven, four failures are due to the first mode and three failures to the second.

VI. Discussion

With the DDHand, we are exploring an underexploited space in hand design. The DDHand aims to improve the transmission of information between the robot and the task. With the deletion of the gearbox and the series spring, the DDHand gains bandwidth, speed, and transparency.

These capabilities are well demonstrated by the smack and snatch task which is hard to realize with conventional grippers. Consider, for example, the Schunk gripper [41] and the Robotiq gripper [36] as examples of geared grippers with strain-gauges and series-elastic actuation, respectively. The Schunk gripper will fail to execute this behavior at the approach phase as it lacks the ability to manage the impulse imparted during collision with the table leading to damage to the fingers or strain-gauge depending on their relative strength. For the Robotiq gripper, the lower stiffness of the passive compliance can manage imparted impulse during the approach phase but the high gear ratio will prevent the fingers to close around the object fast enough to snatch it.

There is still scope to improve the robustness of the smack and snatch grasping behavior with the DDHand. The first of the two failure modes discussed in Section V-C can be resolved by ensuring the table surface is not compliant and prevent the energy transfer to the block or reducing the stiffness of the fingers post-impact. The second failure mode is due to uncertainty of the 2D pose of the block on the table. Better state estimation can lessen the presence of this mode. Integrating intrinsic sensing is also desirable. The fingers can monitor the motor torques during the snatch phase and decelerate the finger that makes contact with the block first.

In this paper, we have discussed the benefits of direct drive actuation for robot hands. It is however essential to address the possible loss of torque that comes with this approach and how to mitigate it. We envision three ways:

Thermal Management: When humans try to pick up something heavier than what we are used to, we either sweat to manage the heat and if that is not enough, we put the thing down briefly. Motors, too, can be driven over their nominal operating limits as long as the temperatures are managed intelligently. This can be done either through active or passive cooling (for example, blowing air over the motors), as in [5, 50], or by intelligent controllers that sense the motor state and take breaks to prevent permanent motor damage, as in [13, 37, 49].

Kinematic Singularities: Another strategy humans employ when carrying heavy things is the use of singularities. For example, while carrying a bag of groceries we tend to lock out our arm straight down to let the structure take most of the weight.

The kinematics of the DDHand finger linkages are nonlinear, and so characteristics such as compliance and force limits vary with operating point (i.e. with the choice of hand pose and grasp configuration). By choosing a hand pose it is possible to put the fingers at singularities or at travel limits to provide high forces, or the opposite to provide high compliance [9].

Directional Rigidity: Conventional manipulators try to be stiff in all directions. Isotropic behavior is an explicit design objective of some grippers, for example Salisbury's milestone design [40]. The conventional approach is essentially a know-nothing approach, reducing the required planning and control intelligence, but also reducing the variety of mechanical intelligence available. Further, universal isotropic stiffness leads to stiff and heavy hands. The DDHand adopts the opposite approach: deliberately anisotropic stiffness. It is rigid in some directions and compliant in others. Specifically, the two degree of freedom fingers are constrained to be planar and can maintain rigidity in the out-of-plane directions (by pushing against the structure and bearings). By intelligently planning grasp and transfer motions, we can achieve lower peak gripping forces.

With these strategies the reduced torque of direct drive can be mitigated, while still maintaining the transparency, force bandwidth, and speed. Grippers like the DDHand can open up new capabilities and behaviors that allow a robot to naturally react to the environment instead of imposing its will on it.

VII. Acknowledgement

References

[1] Agilent. Direct Drive Robot User Guide, March 2014. URL http://www.agilent.com/cs/library/usermanuals/public/G5430-90003_R00_DDRUG_EN.pdf.

[2] D. Alba, M. Armada, and R. Ponticelli. An Introductory Revision to Humanoid Robot Hands. In *Climbing and Walking Robots*, pages 701–712. Springer, Berlin, Heidelberg, 2005. URL http://link.springer.com/10.1007/3-540-29461-9_69.

[3] H. Asada, T. Kanade, and I. Takeyama. Control of a Direct-Drive Arm. *Journal of Dynamic Systems, Measurement, and Control*, 105(3):136, 1983. URL http://DynamicSystems.asmedigitalcollection.asme.org/article.aspx?articleid=1403434.

[4] Haruhiko Asada and Il Hwan Ro. A Linkage Design for Direct-Drive Robot Arms. *Journal of Mechanisms Transmissions and Automation in Design*, 107(4):536, 1985. URL http://MechanicalDesign.asmedigitalcollection.asme.org/article.aspx?articleid=1452647.

[5] Y. Asano, T. Kozuki, S. Ookubo, et al. Human mimetic musculoskeletal humanoid Kengoro toward real world physically interactive actions. In *IEEE International Conference on Humanoid Robots*, pages 876–883, November 2016. doi: 10.1109/HUMANOIDS.2016.7803376.

[6] Antonio Bicchi. Hands for dexterous manipulation and robust grasping: A difficult road toward simplicity. *IEEE Transactions on Robotics and Automation*, 16(6):652–662, 2000. doi: 10.1109/70.897777.

[7] Lionel Birglen and Clement M. Gosselin. Force Analysis of Connected Differential Mechanisms: Application to Grasping. *The International Journal of Robotics Research*, 25(10):1033–1046, 2006.

[8] R. Bischoff, J. Kurth, G. Schreiber, et al. The KUKA-DLR Lightweight Robot arm – a new reference platform for robotics research and manufacturing. In *International Symposium on Robotics and German Conference on Robotics*, pages 1–8, June 2010. URL https://ieeexplore. ieee.org/document/5756872.

[9] J. E. Bobrow, B. Martin, G. Sohl, E. C. Wang, F. C. Park, and Junggon Kim. Optimal robot motions for physical criteria. *Journal of Robotic Systems*, 18(12):785–795, December 2001. URL http://doi.wiley.com/10.1002/rob. 8116.

[10] G. Campion, Qi Wang, and V. Hayward. The Pantograph Mk-II: a haptic instrument. In *2005 IEEE/RSJ International Conference on Intelligent Robots and Systems*, pages 193–198, August 2005. doi: 10.1109/IROS. 2005.1545066. URL https://ieeexplore.ieee.org/document/ 1545066.

[11] Aaron M. Dollar and Robert D. Howe. The highly adaptive SDM hand: Design and performance evaluation. *The International Journal of Robotics Research*, 29(5): 585–597, 2010. URL https://journals.sagepub.com/doi/10. 1177/0278364909360852.

[12] M. Ebner and R.S. Wallace. A direct-drive hand: Design, modeling and control. In *IEEE International Conference on Robotics and Automation*, volume 2, pages 1668–1673, Nagoya, Japan, 1995. IEEE. URL http://ieeexplore.ieee. org/document/525514/.

[13] Kevin C. Galloway, G. C. Haynes, B. Deniz Ilhan, et al. X-RHex: A Highly Mobile Hexapedal Robot for Sensorimotor Tasks. Technical report, University of Pennsylvania, Philadelphia, PA, 2010.

[14] David V. Gealy, Brent McKinley, Stephen Yi, Philipp Wu, Phillip R. Downey, Greg Balke, Allan Zhao, Menglong Guo, Rachel Thomasson, Anthony Sinclair, Peter Cuellar, Zoe McCarthy, and Pieter Abbeel. Quasi-direct drive for low-cost compliant robotic manipulation. In *2019 IEEE International Conference on Robotics and Automation (ICRA)*. IEEE, 2019.

[15] Genesis. Live Drive, October 2017. URL http://www. genesis-robotics.com.

[16] Blake Hannaford. A design framework for teleoperators with kinesthetic feedback. *IEEE Transactions on Robotics and Automation*, 5(4):426–434, 1989.

[17] N. Hogan. Mechanical impedance control in assistive devices and manipulators. In *Joint Automatic Control Conference, Pp. TA10-B*, 1980.

[18] Peter F. Hokayem and Mark W. Spong. Bilateral teleoperation: An historical survey. *Automatica*, 42(12):2035–2057, 2006. URL http://www.sciencedirect.com/science/ article/pii/S0005109806002871.

[19] Jonathan Hurst. Walk this way: To be useful around people, robots need to learn how to move like we do. *IEEE Spectrum*, 56(03):30–51, 2019. URL https://ieeexplore. ieee.org/abstract/document/8651932.

[20] Simon Kalouche. *Design for 3D Agility and Virtual Compliance Using Proprioceptive Force Control in Dynamic Legged Robots*. PhD thesis, Carnegie Mellon University, Pittsburgh, PA, August 2016.

[21] Yukihisa Karako, Shinji Kawakami, Keisuke Koyama, Makoto Shimojo, Taku Senoo, and Masatoshi Ishikawa. High-speed ring insertion by dynamic observable contact hand. In *2019 IEEE International Conference on Robotics and Automation (ICRA)*. IEEE, 2019.

[22] Nathan Kau, Aaron Schultz, Natalie Ferrante, and Patrick Slade. Stanford doggo: An open-source, quasi-direct-drive quadruped. In *2019 IEEE International Conference on Robotics and Automation (ICRA)*. IEEE, 2019.

[23] H. Kazerooni. Direct-drive active compliant end effector (active RCC). *IEEE Journal on Robotics and Automation*, 4(3):324–333, June 1988. ISSN 0882-4967. doi: 10.1109/ 56.793.

[24] Gavin Kenneally, Avik De, and D. E. Koditschek. Design Principles for a Family of Direct-Drive Legged Robots. *IEEE Robotics and Automation Letters*, 1(2):900–907, July 2016. URL http://ieeexplore.ieee.org/document/ 7403902/.

[25] D. A. Lawrence. Stability and transparency in bilateral teleoperation. *IEEE Transactions on Robotics and Automation*, 9(5):624–637, October 1993. URL http: //dx.doi.org/10.1109/70.258054.

[26] R. D. Lorenz, J. J. Zik, and D. J. Sykora. A direct-drive, robot parts, and tooling gripper with high-performance force feedback control. *IEEE Transactions on Industry Applications*, 27(2):275–281, March 1991. ISSN 0093-9994. doi: 10.1109/28.73611.

[27] Kevin M. Lynch and Matthew T. Mason. Dynamic Underactuated Nonprehensile Manipulation. In *IEEE/RSJ International Conference on Intelligent Robots and Systems (IROS)*, pages 889–896, 1996.

[28] R. R. Ma, L. U. Odhner, and A. M. Dollar. A modular, open-source 3D printed underactuated hand. In *2013 IEEE International Conference on Robotics and Automation*, pages 2737–2743, May 2013. doi: 10.1109/ICRA.2013. 6630954.

[29] Matthew T. Mason. Compliance and Force Control for Computer-Controlled Manipulators. *IEEE Trans on Systems, Man, and Cybernetics*, 11(6):418–432, 1981.

[30] Christoph Mittermayer and Andreas Steininger. On the determination of dynamic errors for rise time measurement with an oscilloscope. *IEEE Transactions on Instrumentation and Measurement*, 48(6):1103–1107, 1999.

[31] Gareth J Monkman, Stefan Hesse, Ralf Steinmann, and Henrik Schunk. *Robot Grippers*. John Wiley & Sons, 2007.

[32] A. Namiki, Y. Imai, M. Ishikawa, and M. Kaneko. Development of a high-speed multifingered hand system and its application to catching. In *IEEE/RSJ International Conference on Intelligent Robots and Systems*, volume 3, pages 2666–2671, Las Vegas, Nevada, USA, 2003. IEEE. URL http://ieeexplore.ieee.org/document/1249273/.

[33] G. A. Pratt and M. M. Williamson. Series elastic actuators. In *IEEE/RSJ International Conference on Intelligent Robots and Systems*, volume 1, pages 399–406, Pittsburgh, PA, USA, 1995. IEEE Comput. Soc. Press. URL http://ieeexplore.ieee.org/document/525827/.

[34] Morgan Quigley, Ken Conley, Brian Gerkey, et al. ROS: An open-source Robot Operating System. In *ICRA Workshop on Open Source Software*, 3.2, page 5. Kobe, 2009.

[35] M. H. Raibert and J. J. Craig. Hybrid Position/Force Control of Manipulators. *Transactions of the ASME; Journal of Dynamic Systems, Measurement and Control*, 102, June 1981.

[36] Robotiq. 2F-85 and 2F-140 Grippers. https://robotiq.com/products/2f85-140-adaptive-robot-gripper, 2019. [Online; accessed 20-May-2019].

[37] David Rollinson, Yigit Bilgen, Ben Brown, et al. Design and architecture of a series elastic snake robot. In *IEEE/RSJ International Conference on Intelligent Robots and Systems*, pages 4630–4636, Chicago, IL, USA, September 2014. IEEE. URL http://ieeexplore.ieee.org/document/6943219/.

[38] S. Salcudean and R. L. Hollis. A magnetically levitated fine motion wrist: Kinematics, dynamics and control. In *IEEE International Conference on Robotics and Automation Proceedings*, pages 261–266 vol.1, April 1988. doi: 10.1109/ROBOT.1988.12058.

[39] Septimiu E Salcudean, Ming Zhu, Wen-Hong Zhu, and Keyvan Hashtrudi-Zaad. Transparent bilateral teleoperation under position and rate control. *The International Journal of Robotics Research*, 19(12):1185–1202, 2000.

[40] J Kenneth Salisbury Jr. *Kinematic and Force Analysis of Articulated Hands*. PhD Dissertation, Stanford University, 1982.

[41] SCHUNK GmbH and Co. KG. Wsg gripper, January 2019. URL https://schunk.com/us_en/gripping-systems/series/wsg/.

[42] Sangok Seok, Albert Wang, David Otten, and Sangbae Kim. Actuator design for high force proprioceptive control in fast legged locomotion. In *IEEE/RSJ International Conference on Intelligent Robots and Systems*, pages 1970–1975, Vilamoura-Algarve, Portugal, October 2012. IEEE. URL http://ieeexplore.ieee.org/document/6386252/.

[43] Sangok Seok, Albert Wang, Meng Yee Michael Chuah, et al. Design principles for energy-efficient legged locomotion and implementation on the MIT Cheetah robot. *IEEE/ASME Transactions on Mechatronics*, 20(3):1117–1129, 2015.

[44] Barry Spletzer. Scaling Laws for Mesoscale and Microscale Systems. Technical Report SAND99-2172J, Sandia National Labs., Albuquerque, NM (US); Livermore, CA (US), 1999.

[45] T-Motor. T-Motor GB54-2, October 2017. URL http://store-en.tmotor.com/goods.php?id=445.

[46] TexasInstruments. InstaSPIN BLDC motor control solutions, October 2017. URL http://www.ti.com/instaspin.

[47] W. T. Townsend and J. K. Salisbury. Mechanical bandwidth as a guideline to high-performance manipulator design. In *IEEE International Conference on Robotics and Automation*, pages 1390–1395, Scottsdale, AZ, USA, 1989. IEEE Comput. Soc. Press. URL http://ieeexplore.ieee.org/document/100173/.

[48] Nathan T Ulrich. *Grasping with Mechanical Intelligence*. PhD thesis, University of Pennsylvania, Philadelphia, PA, 1989.

[49] J. Urata, T. Hirose, Y. Namiki, Y. Nakanishi, I. Mizuuchi, and M. Inaba. Thermal control of electrical motors for high-power humanoid robots. In *IEEE/RSJ International Conference on Intelligent Robots and Systems*, pages 2047–2052, September 2008. doi: 10.1109/IROS.2008.4651110.

[50] Junichi Urata and Yuto Nakanishi. Water-cooled motor structure and water-cooled housing, September 2017. URL https://patents.google.com/patent/US9768662B2/en. US Patent.

[51] D. E. Whitney. Force feedback control of manipulator fine motions. *Journal of Dynamic Systems, Measurement, and Control*, 99:91, 1977. URL https://dynamicsystems.asmedigitalcollection.asme.org/article.aspx?articleid=1402627.

[52] D. E. Whitney. Quasi-static assembly of compliantly supported rigid parts. *ASME Journal of Dynamic Systems, Measurement, and Control*, 104:65–77, March 1983.

[53] Michael Zinn, Bernard Roth, Oussama Khatib, and J. Kenneth Salisbury. A New Actuation Approach for Human Friendly Robot Design. *The International Journal of Robotics Research*, 23(4-5):379–398, April 2004. URL http://journals.sagepub.com/doi/10.1177/0278364904042193.